Acta Biomaterialia 38 (2016) 190–200

Contents lists available at ScienceDirect

Acta Biomaterialia

journal homepage: www.elsevier.com/locate/actabiomat

Full length article

Effect of nanolayering of calcium salts of phosphoric acid ester monomers on the durability of resin-dentin bonds

Fu-cong Tian [a,1], Xiao-yan Wang [a,1], Qi Huang [b], Li-na Niu [c,*], Jan Mitchell [d], Zheng-yi Zhang [e], Chandrani Prananik [f], Lu Zhang [a], Ji-hua Chen [c], Lorenzo Breshi [g], David H. Pashley [d], Franklin R. Tay [d,*]

[a] Department of Cariology and Endodontology, School and Hospital of Stomatology, Peking University, Beijing, PR China
[b] Department of Operative Dentistry and Endodontics, Guanghua School of Stomatology, Sun Yat-sen University, Guangzhou, China
[c] State Key Laboratory of Military Stomatology & National Clinical Research Center for Oral Diseases & Shaanxi Key Laboratory of Oral Diseases, Department of Prosthodontics, School of Stomatology, The Fourth Military Medical University, Xi'an, China
[d] The Dental College of Georgia, Augusta University, Augusta, GA, USA
[e] Department of Prosthodontics, School & Hospital of Stomatology, Zhejiang University, Hangzhou, Zhejiang, China
[f] Department of Chemical and Biological Engineering, University of Colorado, Boulder, CO, USA
[g] Department of Biomedical and Neuromotor Sciences, DIBINEM, University of Bologna, Italy

ARTICLE INFO

Article history:
Received 27 January 2016
Received in revised form 13 April 2016
Accepted 19 April 2016
Available online 27 April 2016

Keywords:
10-MDP
Analog
Bond durability
Nanolayering
Organic-inorganic hybrid calcium salt
Phosphoric acid ester resin monomer

ABSTRACT

To investigate the contribution of nanolayering on resin-dentin bond durability, two phosphoric acid ester resin monomers, 10-methacryloyloxy-decyl-dihydrogen-phosphate (10-MDP) or its analog, metha cryloyloxy-penta-propyleneglycol-dihydrogen-phosphate (MDA), were examined for their affinity for mineralized dentin powder in a column chromatography setup. Hydroxyapatite (HA) powder was dispersed in experimental primers consisting of 10-MDP or MDA solvated in ethanol/water and examined with FTIR, ^{31}P MAS-NMR and XPS. Light-curable 10-MDP or MDA primers were used for bonding to dentin, and examined after 24 h or one-year of water-aging by TEM for evidence of nanolayering, and for microtensile bond strength evaluation. Primer-bonded dentin was examined by thin-film XRD to identify short-range order peaks characteristic of nanolayering of resin monomer-Ca salts. Although 10-MDP had better affinity for mineralized dentin than MDA, both monomers completely eluted from the mineralized dentin powder column using ethanol-water as mobile phase, indicating that the adsorption processes were reversible. This finding was supported by chemoanalytic data. XRD of 10-MDP-bonded dentin showed three diffraction peaks hat were absent from MDA-bonded dentin. Nanolayering was identified by TEM in 10-MDP-bonded dentin, but not in MDA-bonded dentin. Significant drop in bond strength (in MPa) was observed for both groups after one-year of water-aging compared with 24-h: 10-MDP group from 48.3 ± 6.3 to 37.4 ± 4.6; MDA group from 50.7 ± 5.0 to 35.7 ± 3.8 ($P < 0.05$), with no significant difference between the two groups at the same time-point. Because both functional monomer-primed, resin-bonded dentin exhibited similar bond strength decline after water-aging, presence of nanolayering is unlikely to contribute to the overall resin-dentin bond durability.

Statement of Significance

The durability of resin-dentin bonds in 10-MDP containing self-etching adhesives has been anecdotally attributed to the presence of nanolayering of 10-MDP-calcium salts in the resin-dentin interface. Results of the present work indicate that such a claim cannot be justified. Complete elution of the phosphoric acid ester monomer from mineralized dentin powder in the column chromatography experiments using ethanol-water mobile phase to simulate the solvent mixture employed in most 10-MDP-containing dentin adhesives further challenges the previously proposed adhesion-decalcification concept that utilizes chemical bonding of phosphoric acid ester monomers to apatite as a bonding mechanism in 10-MDP containing dentin adhesives.

* Corresponding authors at: State Key Laboratory of Military Stomatology & National Clinical Research Center for Oral Diseases & Shaanxi Key Laboratory of Oral Diseases, Department of Prosthodontics, School of Stomatology, The Fourth Military Medical University, Xi'an, Shaanxi, China (L.-n. Niu). The Dental College of Georgia, Augusta University, Augusta, GA 30912-1129, USA (F.R. Tay).
E-mail addresses: niulina831013@126.com (L.-n. Niu), ftay@gru.edu (F.R. Tay).
[1] Equal contributors.

http://dx.doi.org/10.1016/j.actbio.2016.04.034
1742-7061/

1. Introduction

Dentin bonding interfaces degrade with time. Electron microscopy and other *in vitro* tests have provided ultrastructural evidence of degradation in hybrid layers, and decline in resin-dentin bond strengths that resulted from resin hydrolysis and collagen degradation [1,2]. Loss of micromechanical retention between adhesive and dentin eventually leads to clinical restoration failure [3]. Apart from micromechanical interlocking, chemical adhesion between specific functional resin monomers and tooth minerals has been reported as an alternative mechanism for adhesion of methacrylate resins to tooth structures. Chemoanalytic methods have identified prospective chemical reactions that occur in the resin-dentin interface, including adsorption of functional resin molecules on the apatite surface and the formation of resin monomer-calcium salts [4–6].

Due to challenges in quantifying chemical reactions in the resin-dentin interface, a direct link between chemical bonding and resin-dentin bond durability was difficult to be established [7,8]. The water solubility of 10-methacryloyloxydecyl dihydrogen phosphate (10-MDP)-calcium salt was the lowest among salts produced by the reaction between phosphoric acid ester monomers and apatite [5,9,10]. This feature was used to account for the better *in vivo* and *in vitro* dentin bonding results achieved by 10-MDP-containing commercial adhesives [11,12]. In the absence of direct evidence, those long-term *in vivo* and *in vitro* bonding results were used anecdotally as indirect evidence for the contribution of chemical bonding to the overall bonding performance [13]. Because many confounding factors are involved in studies on dentin adhesives, it is taxing to attribute overall bonding performance to the presence of phosphoric acid ester monomer-calcium salts in the resin-dentin interface [14–16].

In 10-MDP primer-treated resin-tooth interfaces, 10-MDP-Ca salts self-assemble into nanolayers, with hypothetical structures consisting of the methacrylate groups of two 10-MDP molecules facing each other, and the functional hydrogen phosphate groups directed away from each other [17]. Ultrastructural manifestation of 10-MDP-Ca nanolayering was corroborated with the appearance of three characteristic peaks in the 2θ range of 2–8° in thin-film X-ray diffraction (XRD) scans of adhesive-coated dentin [18]. These three peaks represent short-range order of the precipitated salts [19]. Based on this finding, several claims have been made for the function of nanolayering in dentin bonding, including protecting collagen fibrils from water-induced degradation due to their hydrophobicity, increasing the resistance of residual apatite crystallites to acidic dissolution, and creating a more gradual transition between the inorganic bonding substrate and the biomaterial [17]. These claims, however, were not supported by experimental evidence.

According to the literature, the propensity of nanolayering formation in resin-dentin adhesives containing phosphoric acid ester monomers is affected by the presence of 2-hydroxyethyl methacrylate (HEMA), agitation, application time, monomer impurity and molecule structure of the phosphoric acid ester monomers [20–22]. These factors, alone or in combination, could have accounted for the paucity of nanolayering in resin-dentin interfaces created by commercial 10-MDP-containing adhesives [19]. Other functional resin monomers with similar structure as 10-MDP have also been investigated [10,23,24]. These monomers contain different hydrocarbon or fluorocarbon chains as spacer group between the methacrylate group and the phosphate group. The spacer group is known to influence monomer characteristics such as flexibility, solubility, hydrophobicity, viscosity, and wetting behavior. Long spacers are used to avoid steric hindrance during polymerization and to enhance mechanical properties [25]. These functional resin monomers were tested for their calcium salt solubility, chemical shifts after reacting with hydroxyapatite or powdered enamel and dentin with nuclear magnetic resonance (NMR) spectroscopy, bond strength and ultrastructural examination of the resin-dentin interface. Many of them produce nanolayering patterns with varying interlayer thickness. However, none of these studies was able to elucidate whether the presence of nanolayering was responsible for the durability of resin-dentin bonds.

To circumvent the problem of interference of other methacrylate resin monomers on nanolayering formation, 10-MDP and a new 10-MDP analog with a different spacer group were respectively used as the only resin monomer for creating experimental self-etching dentin adhesives. The analog member had been tested in a pilot study to confirm the absence of nanolayering when bonded to dentin, and served as the control analog for 10-MDP. This enabled the authors to evaluate the contribution of nanolayering to the longevity of resin-dentin bonds. The interactions between the two resin monomers and the dentin mineral phase were first investigated, followed by their influences on dentin bonding performance. The first null hypothesis tested was that there is no difference in the affinity of 10-MDP and the analog resin monomer for mineralized dentin. The second null hypothesis tested was that there is no difference in the capability of both phosphoric acid ester monomers to produce nanolayering on the dentin surface. The third null hypothesis tested was that nanolayering of phosphoric acid ester monomer-calcium salts is unstable after water aging and does not contribute to the resin-dentin bond durability.

2. Materials and methods

2.1. Materials

Sixty non-carious human third molars were used in the present study. The use of human teeth for research was approved by the Human Assurance Committee of the Augusta University, Georgia. The teeth were refrigerated at 4 °C in 0.9% NaCl that contained 0.02% sodium azide to prevent bacterial growth.

The two phosphoric acid ester monomers examined were: 10-MDP (molar mass: 322.35 g/mol) and methacryloyloxy-penta-propyleneglycol-dihydrogen-phosphate (10-MDP analog, designated as "MDA"; molar mass: 456.48 g/mol). The molecule structures of the two resin monomers are illustrated in Fig. 1. Both resin monomers were obtained from DM Healthcare Products, Inc. (San Diego, CA, USA). 2-hydroxyethyl methacrylate (HEMA; molar mass: 130.14 g/mol) and hydroxyapatite (HA; particle size ~200 nm) were obtained from MilliporeSigma (St Louis, MO, USA).

Two experimental primers were prepared by blending 10-MDP or MDA with ethanol and water in the ratio of 15:45:40 wt% [20]. For primers used in dentin bonding as part of the experimental adhesive systems, camphorquinone (CQ; 1 wt%) and ethyl-4-dimethylamino benzoate (EDMAB; 0.4 wt%), both from MilliporeSigma, were added to render the primers light-curable. The pH values of the experimental primer solutions (measured with a pH meter, Orion Star A211, ThermoScientific, Waltham, MA, USA) were 2.65 for the primer containing 10-MDP, and 2.38 for the primer containing 10-MDP analog.

2.2. Affinity of the two phosphoric acid ester monomers for mineralized dentin

A modified hydroxyapatite column chromatography procedure [26] was adopted in the present study to examine the elution characteristics of the two phosphoric acid ester monomers in the presence of mineralized dentin powder, as a measure of the affinity of

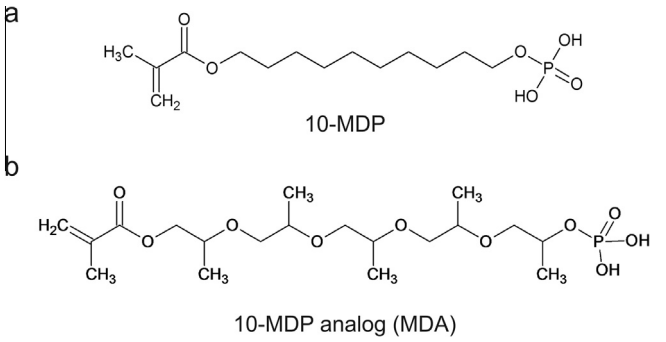

Fig. 1. Molecular structure of the acid phosphoric acid ester monomers employed in the present study. a. 10-MDP. b. 10-MDP analog (MDA).

the resin monomers for dentin apatite. Six hundred freshly extracted bovine incisors were obtained, stored in 0.9% NaCl with 0.02% sodium azide and used within one month after extraction. Bovine dentin powder (particle size 300–500 μm) was prepared according to the authors' previous protocol [27]. The mineralized dentin powder was packed into a 1 cm diameter × 30 cm long glass column. Specifically, 24.1 g bovine dentin powder was packed to 25 cm of the length of the column to form the stationary phase. Three kinds of liquid media were employed as the mobile phases: pure ethanol, ethanol and water mixture (9:8 weight ratio) and salt buffer (0.02 M Tris-HCl and 0.15 M NaCl dissolved in 1 L water, pH 7.4, both from MilliporeSigma). Each liquid medium was added to the column to reach the surface of the packed stationary phase. The flow rate of each mobile phase was set to 14.4 mL/h to elute the column, which was controlled by a precision syringe pump. Elution liquid was collected at 5 min interval in 1.2 mL aliquots.

Three tracers were analyzed: 10-MDP (0.5 mg/mL), MDA (0.5 mg/mL) and HEMA (0.125 mg/mL, used as non-adsorption control for mineralized dentin). The solvent for the tracers were the same as the mobile phase used for eluting the column. Because 10-MDP was only sparingly water-soluble, 5% ethanol was used as a co-solvent in preparing 10-MDP tracer and MDA tracer in the salt buffer. Unlike traditional hydroxyapatite column chromatography, only one tracer was added at one time, to investigate the affinity of each tracer in different mobile phases with mineralized dentin (i.e. the stationary phase). Because both acidic resin monomers can partially demineralize dentin, fresh dentin powder was used in the column for evaluation of each tracer dissolved in each mobile phase. Spectrophotometric absorbance of the eluent was monitored at 220 nm after addition of 0.5 mL tracer solution to the column, with simultaneous fraction collection of the mobile phase. The volume of the elution fraction was calculated by dividing the weight of the fraction contents by density of the solvent. The relationship between spectrophotometric absorption and elution volume was used to generate an elution profile of the resin monomer for the corresponding mobile phase. The eluted amount of tracer was quantified using linear regression equations that correlated absorbance at 220 nm with known tracer concentrations. The eluted tracer amount was then multiplied by the respective fraction volume to obtain the exact amount of tracer resin monomer in the fraction. The total percentage recovery of the eluted tracer was calculated cumulatively from each fraction divided by the volume of the eluent. Each tracer dissolved in a particular mobile phase was run in the column for three times to get repeatable results.

2.3. Chemoanalytic characterization of resin monomer-apatite interaction

Hydroxyapatite powder (0.4 g) was dispersed in 2 g of the non-polymerizable version of each experimental primer at ambient temperature for 2 h with constant stirring. The suspension was centrifuged and decanted to retrieve the resin monomer-coated HA particles. The retrieved HA particles were washed with absolute ethanol for three times and dried in open air at ambient temperature for 48 h. The dried solids were examined by Fourier transform infrared spectroscopy (FTIR), ^{31}P solid-state NMR and X-ray photoelectron spectroscopy (XPS). Untreated HA powder was used as control.

Infrared spectra was recorded between the spectral range of 4000–400 cm^{-1} using a FTIR spectrometer (Nicolet 6700; ThermoScientific, Waltham, MA) with an attenuated total reflection setup at 4 cm^{-1} resolution and 32 scans. ^{31}P solid-state NMR was performed using a Tecmag-based console (Tecmag Inc., Houston, TX, USA) on an Oxford 363 MHz spectrometer (Oxford Instruments, Oxfordshire, United Kingdom) equipped with a 7 mm Magic Angle Spinning (MAS) probe, at a frequency of 147.085 MHz, using a 45° pulse length and a 60 s recycle delay. Specimens were spun at 6.6 kHz, using 40 scans per specimen. Chemicals shifts were referenced to crystalline H_3PO_4 powder at 0.0 ppm.

For XPS, 15 wt% solutions of each resin monomer (10-MDP or MDA) were dissolved in ethanol or water, with addition of photoinitiator. One millimeter-thick HA plates (Clarkson Chromatography Products Inc., South Williamsport, PA, USA) were treated with each solution for 30 s or 30 min, followed by ultrasonication twice in ethanol for 20 min. The phosphoric acid ester monomer-treated HA plates were analyzed (ESCALab 250Xi, ThermoScientific) using 200 W monochromated Al Kα radiation. A 500 μm X-ray spot was used for XPS analysis. The base pressure in the analysis chamber was 3×10^{-8} Pa. The hydrocarbon C 1s line at 284.8 eV from adventitious carbon was used for energy referencing. Wide (survey spectra) and narrow scans were recorded at a pass energy of 80 and 40 eV, respectively. Quantitative data were obtained from peak areas.

2.4. Contact angle measurement

Twelve 1 mm-thick mid-coronal human dentin disks were prepared by sectioning perpendicularly to the longitudinal axis of each tooth using a low-speed diamond saw (Isomet, Buehler Ltd, USA) with water cooling. The dentin surfaces were wet-polished with 600 grit silicon carbide paper for 1 min, kept in water and air-dried within 5 s before use to avoid desiccation. To measure changes in the contact angle of water on the experimental primer-treated dentin surfaces, untreated dentin disks were used as the baseline control. Six disks were employed for each experimental primer (N = 6; untreated dentin discs were re-used for priming dentin). Each primer was applied on the dentin surface for 20 s with agitation, air-dried and light-cured for 20 s using a Light Emitting Diode light-curing unit (Valo, Ultradent, South Jordan, UT, USA) with an output density of 500 mW/cm^2. A Mylar sheet was used to cover the primed surface during light-curing to eliminate creating an oxygen inhibition layer on the cured surface. For each cured surface, the static contact angle was measured (EasyDrop DSA30, Kruss, Hamburg, Germany) using a 5 μL water drop. Four hundred frames collected during the first 3 min were used to calculate the average contact angle.

Contact angles obtained before primer treatment, after 10-MDP primer treatment and after MDA primer treatment were statistically analyzed using one-factor analysis of variance (ANOVA) after ascertaining that the normality (Shapiro-Wilk test) and equal variance (modified Levene test) assumptions of the data set were not violated. Post-hoc pairwise comparisons were conducted using the Holm-Sidak statistic. Statistical significance was set at $\alpha = 0.05$.

2.5. Microtensile bond strength evaluation

Forty human third molars were used for this part of the study (N = 10 for each experimental primer and each of the two aging periods). Using the procedures described in Section 2.4, 3-mm thick coronal dentin blocks were prepared with the bonding surface residing in mid-coronal dentin. Each experimental primer was applied on dentin surface for 20 s with agitation, air-dried, coated with a layer of unfilled, phosphoric acid ester monomer-free resin adhesive (DE Bonding Resin, Bisco, Inc., Schaumburg, IL, USA) and light-cured for 20 s. Two 2-mm thick layers of a hybrid resin composite (Clearfil AP-X, Kuraray, Tokyo, Japan) were placed over the bonded surface. Each layer was light-cured individually for 40 s. After storing in 37 °C water for 24 h or one year (with storage media changed weekly), each bonded tooth was vertically sectioned into 0.9 mm thick slabs. The center slab was saved for transmission electron microscopy (TEM), as described in the subsequent section. The two adjacent slabs were sectioned into 0.9 mm × 0.9 mm beams; the central beams with enough dentin length for testing from each slab were used for microtensile bond strength testing. Thus, for each experimental primer and each aging period, twenty beams containing the resin-dentin interface (one beam per slab × two slabs per tooth × ten teeth) were used for microtensile bond testing. Because beams obtained from the same tooth cannot be considered independent specimens without increasing variation in adhesive resistance, each tooth should be considered a statistical unit and mean values obtained from all specimens derived from the same tooth should be analyzed [28]. Accordingly, bond strength values derived from the two beams of the same tooth was averaged and the resultant value was used to represent the bond strength of that tooth. For each group, ten values obtained from ten teeth were used for determining the mean bond strength representative of that group (N = 10). Each beam was glued to a testing jig and stressed to failure under tension using a universal testing machine (Vitrodyne V1000, Liveco Inc, Burlington, VT, USA) at cross-head speed of 1 mm/min. Failure modes were examined under a stereoscopic microscope and classified as adhesive failure (A, failure along the adhesive interface), mixed failure (M, failure within the adhesive joint together with failure within the resin composite or dentin), or cohesive failure (C, failure within the resin composite or dentin).

Statistical analysis was conducted with two-factor analysis of variance to examine the effects of the two experimental primers and the two aging periods, and the interaction of those two factors on tensile bond strength. The two strength values from one tooth were treated as statistically-dependent. Post-hoc pairwise comparisons were performed using the Holm-Sidak statistic. Parametric statistical methods were employed under the premise that the normality and equal variance assumptions of the data sets were not violated. Statistical significance was set at $\alpha = 0.05$.

2.6. Transmission electron microscopy of the resin-dentin interface

Six specimens were randomly selected from the ten central slabs of each group (N = 6), as described in the previous section. A 0.9 mm × 0.9 mm beam was prepared from each selected slab. The beams were dehydrated in an ascending ethanol series (50–100%), immersed in propylene oxide as transition medium, and embedded in epoxy resin. Ninety nanometer-thick sections were prepared using an ultramicrotome and examined without staining, using a JEM-1230 TEM (JEOL, Tokyo, Japan) at 110 kV.

2.7. X-ray diffraction of primed dentin

Eight human teeth (four for each experimental primer) were used for thin-film X-ray diffraction (XRD). Each primer was applied to a 1-mm thick dentin surface for 20 s with agitation, air-dried and left uncured. The specimens were examined with thin-film XRD (CuKα XRD; d/max2500, Rigaku, Tokyo, Japan) at 40 kV and 200 mA. The incident beam angle was kept low and fixed at 1.0°. A scanning time of 0.02°/sec was employed for 2θ scan from 0.6° to 40°.

3. Results

3.1. Affinity for mineralized dentin

Irrespective of the mobile phase, the elution profiles of the control HEMA tracer exhibited maximal elution at around 10 mL, with a retention of about 40 min. The HEMA tracer was almost completely recovered from the mineralized dentin column (Fig. 2a). For the 10-MDP tracer, double peaks were observed in the elution profiles of resin monomer in ethanol-water or salt buffer. The first peak appeared at around 12 mL, and the second peak appeared at around 24 mL. Appearance of the first peak in the elution profiles of all 3 mobile phases is indicative of the presence of low molecule weight impurities in the commercial source of 10-MDP; this impurity had no affinity for mineralized dentin and were rapidly eluded from the dentin column. Appearance of the second peak with different peak heights is indicative of different extents of irreversible affinity of 10-MDP in different solvents with mineralized dentin. The recovery rate of 10-MDP from the mineralized dentin column were 100%, 36.5% and 18.9% for the ethanol-water mixture, salt buffer and ethanol mobile phases, respectively (Fig. 2b). Similar to HEMA, the elution profiles of the MDA resin monomer also exhibited peak elution at approximately 10 mL. When dissolved in ethanol-water, the elution profile was skewed toward the right, with prolonged, reversible affinity of the resin monomer for mineralized dentin. Compared to 100% elution of MDA when the resin monomer was dissolved in the ethanol-water mixture or salt buffer, only one third of the MDA eluded from dentin column when it was dissolved in ethanol, which is indicative of irreversible affinity of ethanol-solvated MDA with mineralized dentin (Fig. 2c).

3.2. Chemoanalytic characterization of resin monomer-apatite interaction

Although absorbance peaks characteristic of the phosphate functional group in 10-MDP and MDA were detected by FTIR, those peaks overlapped with the HA phosphate peaks [29] in 10-MDP-treated HA and MDA-treated HA. Hence, definitive conclusions could not be established regarding the affinity of those resin monomers for HA. By contrast, the C═O stretching vibration (1716 cm^{-1}) of the methacryloxy carbonyl group [10] was detected from the two neat resin monomers (Fig. 3a for 10-MDP; Fig. 3b for MDA) but not from untreated HA. After reaction of the respective resin monomer with HA and rigorous rinsing with ethanol, the methacryloxy carbonyl peak was retained in 10-MDP-treated HA but disappeared from MDA-treated HA.

^{31}P MAS NMR of HA (Fig. 3c) showed an intense peak at 2.676 ppm that is assigned to the PO_4^{3-} group of hydroxyapatite [30]. After the HA was treated with MDA for 2 h, a new peak emerged at 1.498 ppm, that may be assigned to $CaHPO_4{\cdot}2H_2O$ [29]. The aforementioned peak was absent when HA was treated with 10-MDP for 2 h. Instead, a low-intensity peak appeared at 0.6 to −0.8 ppm that may be assigned to 10-MDP-Ca salt formation [17]. The peak at −5.22 to −7.68 ppm may be attributed to the formation of pyrophosphate on the HA surface after its interaction with 10-MDP [31]. The hydroxyapatite PO_4^{3-} peak shifted slightly to the right (2.516 ppm) for the 10-MDP-treated specimen, and to the left (2.842 ppm) for the MDA-treated specimen.

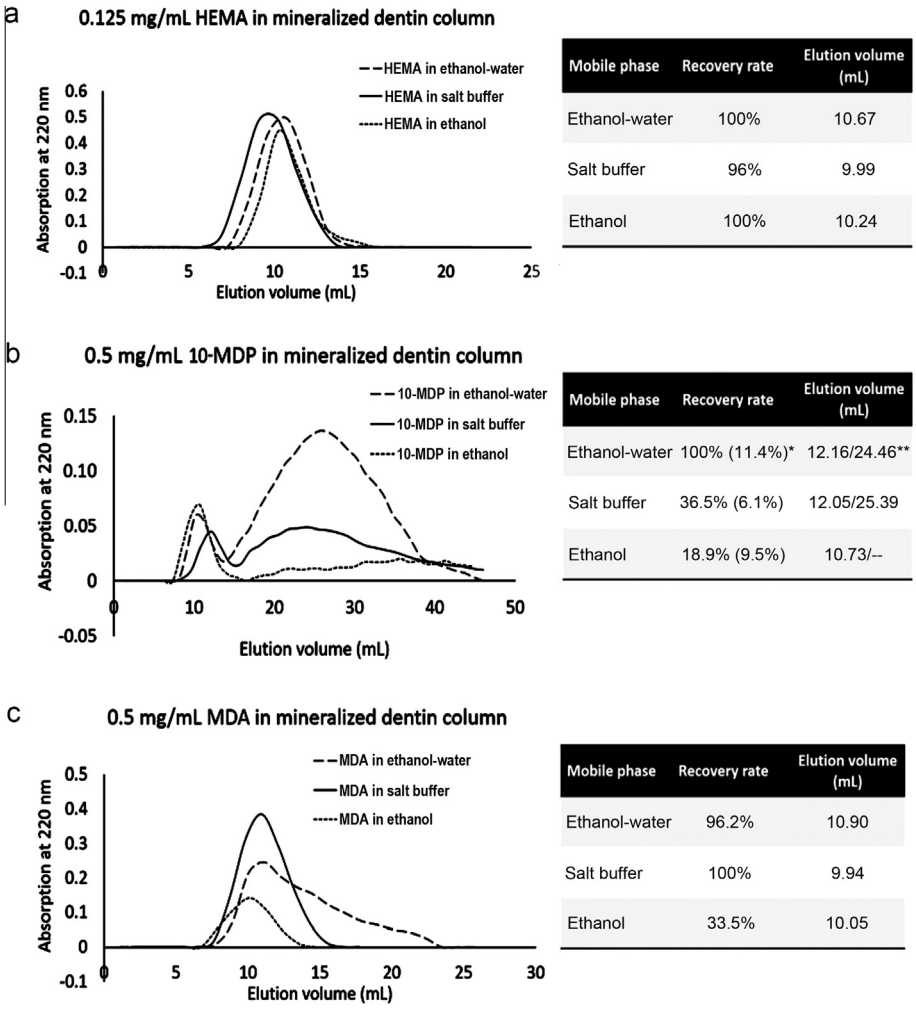

Mobile phase	Recovery rate	Elution volume (mL)
Ethanol-water	100%	10.67
Salt buffer	96%	9.99
Ethanol	100%	10.24

Mobile phase	Recovery rate	Elution volume (mL)
Ethanol-water	100% (11.4%)*	12.16/24.46**
Salt buffer	36.5% (6.1%)	12.05/25.39
Ethanol	18.9% (9.5%)	10.73/--

Mobile phase	Recovery rate	Elution volume (mL)
Ethanol-water	96.2%	10.90
Salt buffer	100%	9.94
Ethanol	33.5%	10.05

Fig. 2. Elution profile of different tracers from mineralized dentin columns. a. Elution profile of 0.125 mg/mL HEMA (control). Table showed recovery rate and elution volume of HEMA from the 3 mobile phases ethanol-water mixture, salt buffer and pure ethanol. b. Elution profile of 0.5 mg/mL 10-MDP showed double peaks (may be caused by impurities) and prolonged elution of the 2nd peak compared to the control. Table showed recovery rate and elution volume of 10-MDP from different mobile phases (*number in parenthesis indicate recovery rate of the first peak containing impurities other than 10-MDP; **numbers indicate elution volumes of first and second peaks). c. Elution profile of 0.5 mg/mL MDA showed asymmetrical peak in ethanol-water mixture. Table showed recovery rate and elution volume of MDA from different mobile phases.

For XPS, quantitative data of the atom% were obtained from peak areas derived from the O 1s, Ca 2p, P 2p and C 1s, from which the Ca/P, O/Ca and C/Ca ratios were calculated (Table 1). The Ca/P ratios were substantially lower for 10-MDP treated HA (both 30 s and 30 min treatment) that may be attributed to the increase in P percentage after resin monomer adsorption to HA; only minimal lowering the Ca/P ratios were identified from MDA-treated HA. The C/Ca and O/Ca ratios increased for 10-MDP treated HA as early as 30 s when compared to the untreated HA, suggesting that there was adsorbed10-MDP on HA. The C/Ca and O/Ca ratios showed slight drop for 10-MDP and slight increase for MDA after 30 min reaction compared to the 30 s spectra. The Ca 2p (Ca $2p_{1/2}$ at 350.67 eV and Ca $2p_{3/2}$ at 347.12 eV) and P 2p (133.22 eV) narrow scans of HA did not exhibit significant shifts after the HA was treated with 10-MDP or MDA. The C1 s narrow scan spectrum was also identified from the commercial source of HA (Fig. 3d), with a major deconvoluted C—C peak at 284.80 eV, a C—O peak at 286.2 eV, a —COO peak at 288.1 eV and a small hydrocarbonate peak 289.5 eV [32], that may be attributed to the adsorption of adventitious hydrocarbon impurities and incorporation of CO_2 in the air and solutions during synthesis [33]. These carbon-related peaks are frequently identified from commercially available synthetic hydroxyapatite [34]. The C—C and C—O peaks in HA were almost identical with similar peaks identified from the C 1s narrow scans of 10-MDP [5] and MDA monomer. In addition, a —COO ester peak was present at ~288.7 eV for the 10-MDP [5] and MDA monomer (not shown). This —COO peak appeared in the C 1s narrow scans of HA that had been treated with 10-MDP for either 30 s or 30 min (Fig. 3e). A similar —COO ester peak associated with MDA adsorption was initially observed when HA was treated with MDA for 30 s; however, this peak was no longer observed after HA was treated with MDA for 30 min (Fig. 3f).

3.3. Contact angles

Significant difference was detected from the contact angle data ($P < 0.05$). Contact angle of water on dentin surface before primer treatment was 25.03° ± 6.12°, which was significantly lower than the 45.32° ± 2.58° obtained for 10-MDP primed dentin ($P < 0.05$), and the 32.23° ± 6.07° obtained for MDA-primed dentin ($P < 0.05$). The 10-MDP primed dentin surface was significantly more hydrophobic than the MDA-primed dentin surface ($P < 0.05$).

3.4. Microtensile bond strengths

Tensile bond strengths (means ± standard mediations) for dentin bonded with the 10-MDP-containing experimental primer were 48.3 ± 6.3 MPa after 24 h of water storage, and 37.4 ± 4.6 MPa after

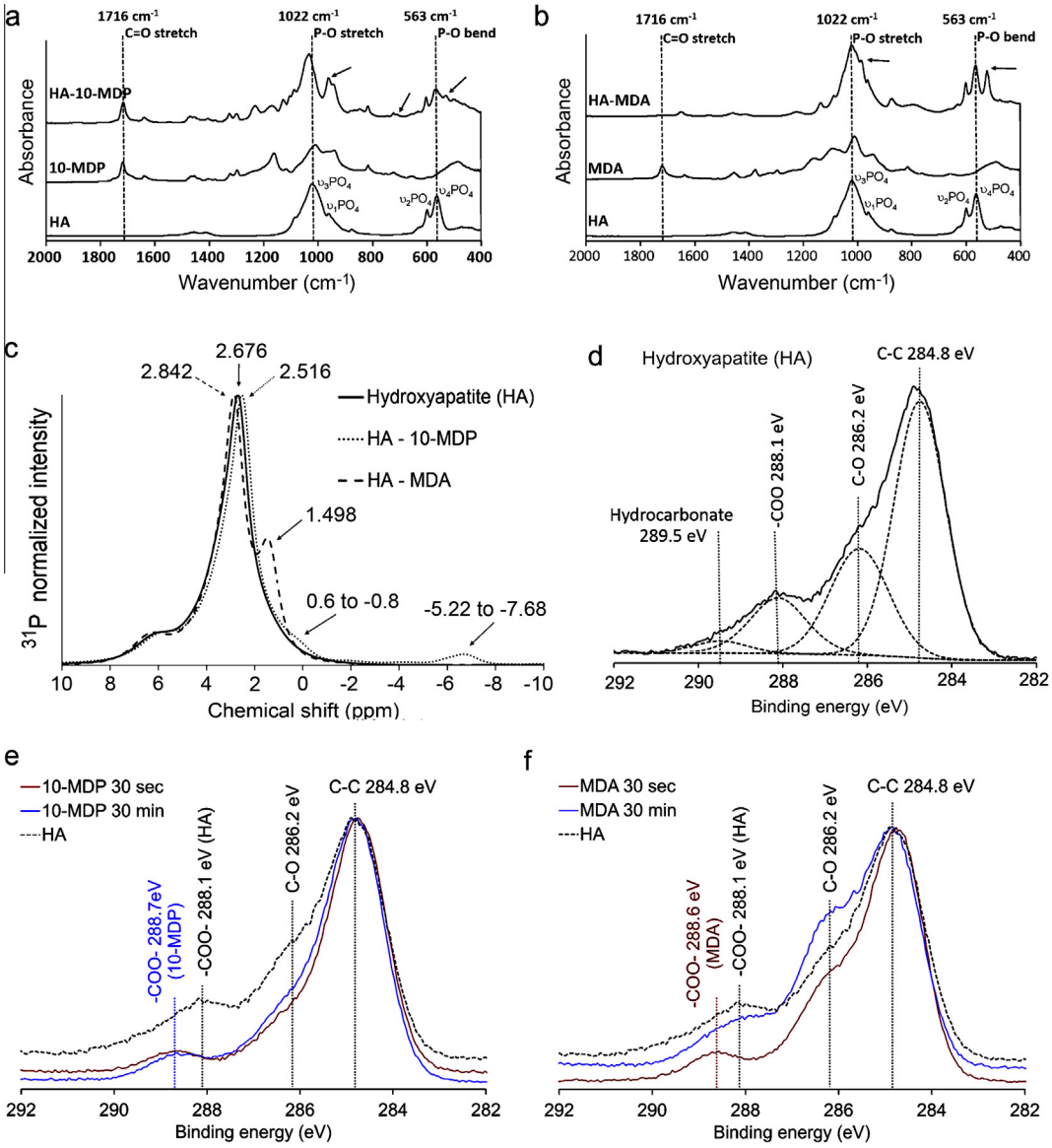

Fig. 3. Chemoanalytic characterization of the interaction between the two phosphoric acid ester monomers with hydroxyapatite (HA). a. FTIR spectra of HA, neat 10-MDP primer and 10-MDP primer-treated HA after ethanol washing. b. FTIR spectra of HA, neat MDA primer and MDA primer-treated HA after ethanol washing. For both a and b, arrows indicate emergence of new phosphate peaks following treatment of HA with the respective resin monomer. c. ^{31}P MAS-NMR. Superimposition of the major P peak in hydroxyapatite (HA), 10-MDP primer-treated HA (HA – 10-MDP) and MDA primer-treated HA (HA – MDA). d. XPS narrow-scan spectrum of the C 1s region in untreated HA. e. Superimpositions of XPS narrow-scan spectrum of the C 1s regions of untreated HA and HA treated with 10-MDP primer for 30 s or 30 min (peak deconvolutions not shown). f. Superimpositions of XPS narrow-scan spectrum of the C 1s regions of untreated HA and HA treated with MDA primer for 30 s or 30 min (peak deconvolutions not shown).

Table 1
Atom percentage ratio of hydroxyapatite (HA) treated with 10-MDP or 10-MDP analog (MDA) resin monomer derived from XPS analysis.

Atomic% ratio	Untreated HA	10-MDP		MDA	
		30 s	30 min	30 s	30 min
Ca/P	1.35	1.06	1.08	1.27	1.26
C/Ca	1.79	4.73	4.35	1.94	2.67
O/Ca	3.41	4.16	3.88	3.13	3.49

one year of water-aging. Those for dentin bonded with the MDA-containing experimental primer were 50.7 ± 5.0 MPa after 24 h and 35.7 ± 3.8 MPa after one year. Significant difference was identified for the factor "aging period" ($P < 0.001$) but not for the factor "experimental primer" ($P = 0.791$). The interaction of those two factors was not statistically significant ($P = 0.070$). Post-hoc pairwise comparisons indicated that for the factor "aging period", significant differences in the bond strength data between 24 h and one year was detected for MDA ($P < 0.001$) and 10-MDP ($P < 0.001$). For the factor "experimental primer", no significant difference in the bond strength data between MDA and 10-MDP was detected after 24 h ($P = 0.141$) or after one year ($P = 0.269$). Failure mode distribution (in the order: adhesive failure/mixed failure/cohesive failure) was 1/15/4 for the MDP immediate group, 2/15/3 for the MDA immediate group, 2/18/0 for the MDP one-year group and 4/15/1 for the MDA one year group. For all subgroups, mixed failure was the predominant failure mode.

3.5. Transmission electron microscopy

Unstained, non-demineralized sections of the 10-MDP primer-treated dentin interface after 24 h of water storage showed a 0.5–1 μm thick hybrid layer with a gray layer produced by the

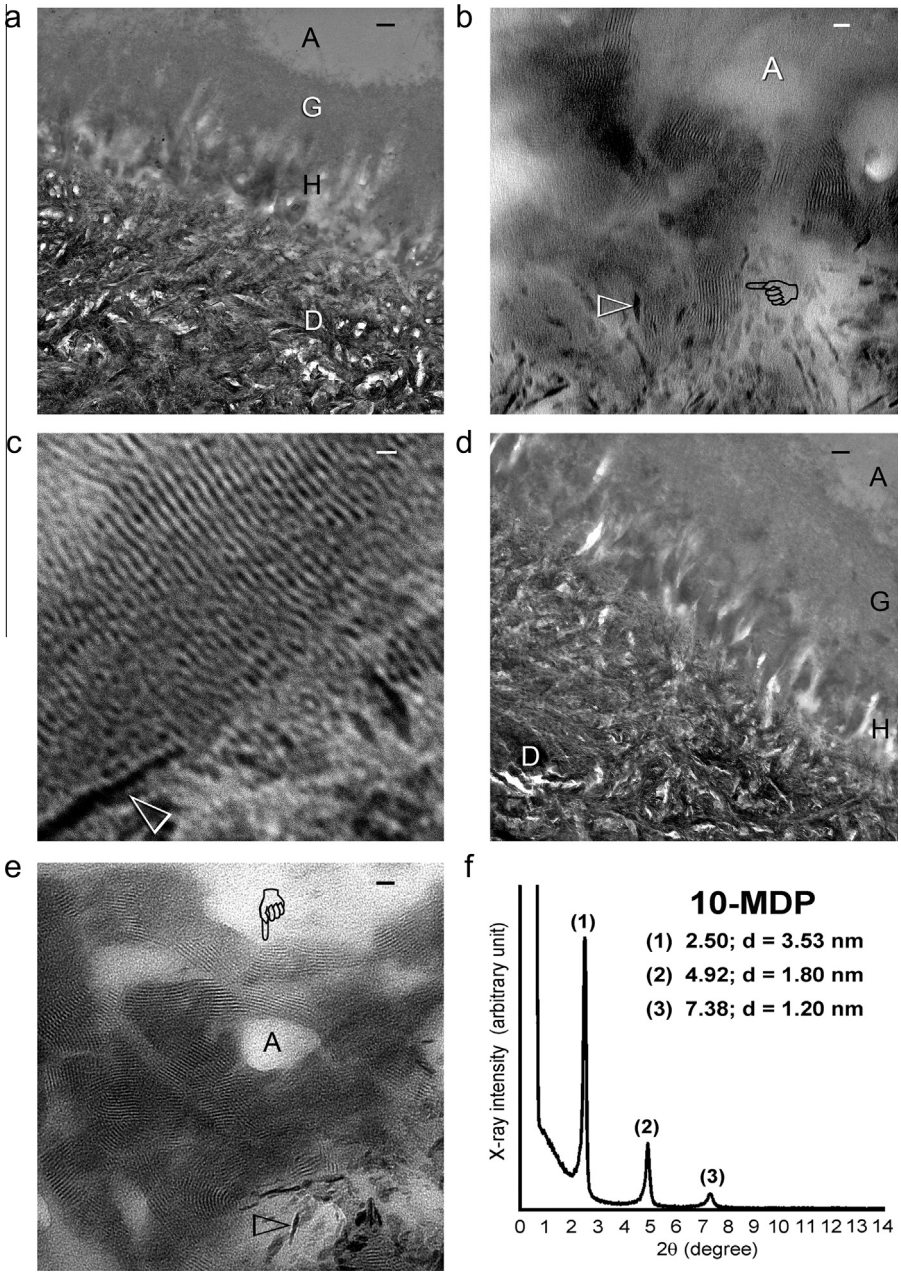

Fig. 4. TEM images of unstained, non-demineralized sections of the resin-dentin interface (a-e) and XRD spectrum (f) created by 15% 10-MDP primer-bonded human dentin. Abbreviations: A: adhesive; G: gray layer of 10-MDP-Ca salt deposits; H: 0.5–1 μm thick hybrid layer created by the self-etching primer; D; mineralized dentin. a. Low magnification after 24 h of water storage. Bar = 200 nm. b. High magnification of the 24-h resin-dentin interface showing nanolayering (pointer) and remnant apatite crystallites (open arrowhead) in the hybrid layer. Nanolayering is profusely observed within the mineral salt layer. Bar = 20 nm. c. Very high magnification of the nanolayering structure in b. Bar = 5 nm. d. Low magnification after 1 year of water storage. Bar = 200 nm. e. High magnification of the 1-year resin-dentin interface showing retained nanolayering (pointer) on top of remnant apatite crystallites (open arrowhead). Bar = 20 nm. f. Thin film-XRD spectrum from 2° to 14° 2θ, created by the application of the 10-MDP primer on dentin. Three small peaks derived from 10-MDP-Ca salts are visible, with their corresponding reflection angles and calculated d-spacings.

deposition of resin monomer-calcium salts on top of the hybrid layer (Fig. 4a). At higher magnification, profuse nanolayering could be identified within the gray layer (Fig. 4b). Some of the electron-dense nanolayers were associated with remnant apatite crystallites in the hybrid layer. At very high magnification, the nanolayers were between 3.5 and 4 nm thick (Fig. 4c). After one year of aging in water, nanolayering could still be identified from the dentin surface of the 10-MDP primer-treated dentin (Fig. 4d and e).

Unstained, non-demineralized sections of the MDA primer-treated dentin interface after 24 h of water storage showed a 0.5–1 μm thick hybrid layer with no evidence of resin monomer-calcium salt deposition (Fig. 5a). At higher magnification, no nanolayering could be identified around the remnant apatite crystallites on the surface of the hybrid layer (Fig. 5b). Similar features were observed (i.e. absence of nanolayering) in the images taken of the MDA primer-treated dentin after one year of water aging (Fig. 5c and d).

3.6. X-ray diffraction

Thin-film glancing-angle XRD spectra of the dentin surface after self-etching with the experimental 10-MDP primer showed three characteristic diffraction peaks present on the 15% 10-MDP primer-treated dentin surface (Fig. 4f, $2\theta = 2.50°$, 4.92°, 7.38°).

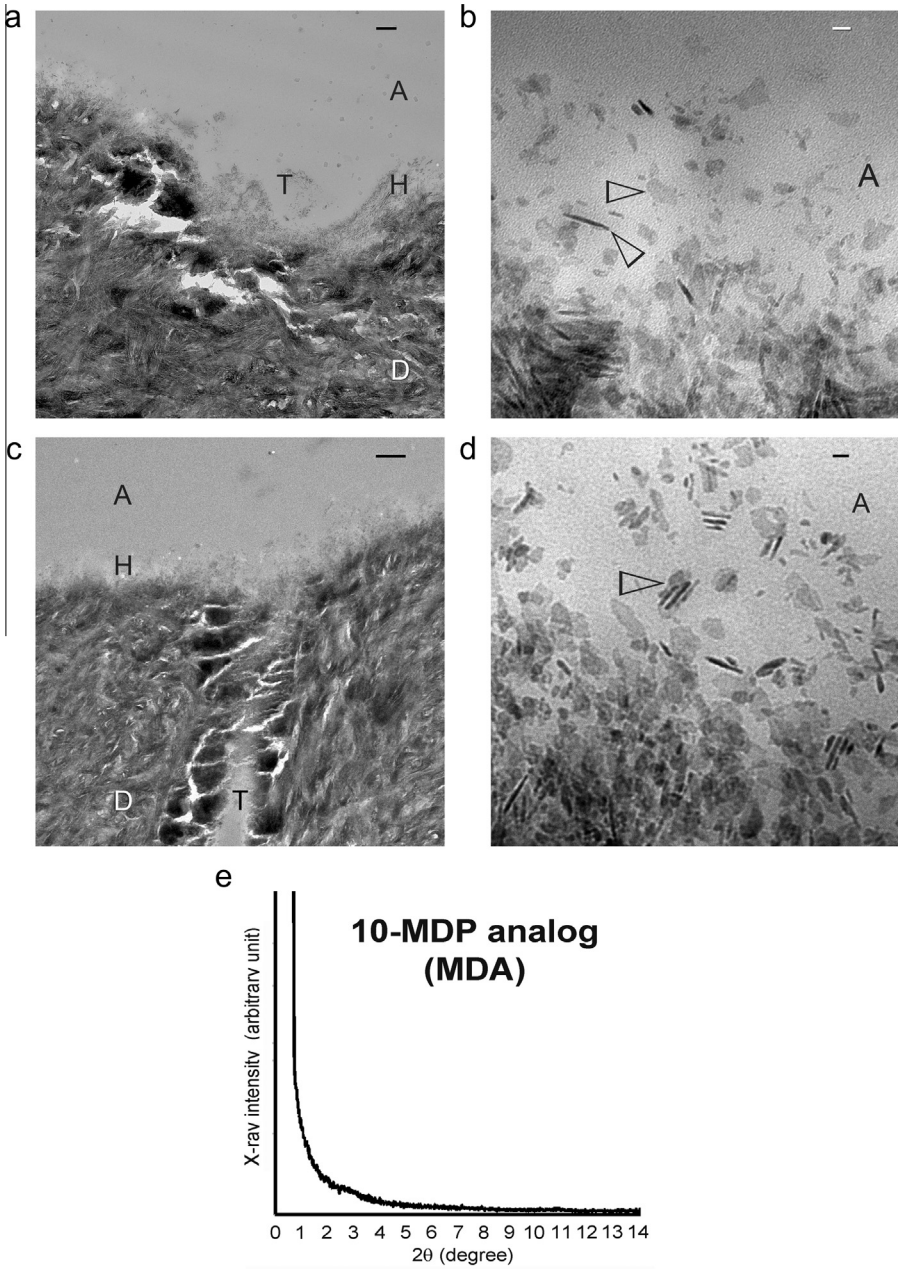

Fig. 5. TEM images of unstained, non-demineralized sections of the resin-dentin interface (a-d) and XRD spectrum (e) created by 15% MDA primer-bonded human dentin. Abbreviations: A: adhesive; H: 0.5–1 μm thick hybrid layer; D; mineralized dentin. T: dentinal tubule. a. Low magnification after 24 h of water storage. No gray deposits could be identified on top of the hybrid layer. Bar = 200 nm. b. High magnification of the 24-h resin-dentin interface showing absence of nanolayering. Open arrowheads: remnant apatite crystallites. Bar = 20 nm. c. Low magnification after 1 year of water storage. Bar = 500 nm. d. High magnification of the 1-year resin-dentin interface showing absence of nanolayering in the resin-dentin interface. Open arrowhead: remnant apatite crystallites. Bar = 20 nm. e. Thin film-XRD spectrum from 2° to 14° 2θ, created by the application of the MDA primer on dentin. No peaks characteristic of short-range order can be identified.

These peaks were absent in the XRD spectrum of the MDA primer-treated dentin surface (Fig. 5e).

4. Discussion

Ideally, studies on the contribution of nanolayering of Ca-resin monomer salts to the longevity of resin-dentin bonds should be contemplated using commercial self-etching adhesives [35]. Because HEMA is present in most 10-MDP-containing self-etching adhesives [19] and HEMA inhibits interfacial nanolayering of the functional monomer 10-MDP [21], nanolayering is rarely identified from the resin-dentin interface of bonds created by commercialized 10-MDP-containing self-etching adhesives [19]. Hence, the authors have to resort to using experimental primers containing only the functional resin monomers to accomplish their objectives. The use of similar experimental primers had been shown to produce immediate resin-dentin bond strength that was similar to the use of commercial 10-MDP-containing adhesives [20].

Based on the present results, the first null hypothesis that "there is no difference in the affinity of 10-MDP and the analog resin monomer for mineralized dentin" has to be rejected. In the column chromatography experiments with ethanol-water mixture as the mobile phase, the retention time of 10-MDP in the mineral-

ized dentin column was about 2 h *vs* 1 h for the 10-MDP analog (i.e. MDA) and HEMA. This implies that 10-MDP has better affinity for apatite than its analog. The use of ethanol-water mixture as the mobile phase was to simulate the solvent vehicle in most commercially available 10-MDP-containing adhesives. Because both ethanol-water solvated 10-MDP and MDA were almost completely recovered from the column after 3 h of elution, the interactions between these phosphoric acid ester monomers and apatite are most likely to be reversible in nature.

The mineralized bovine dentin powder column chromatography setup in the present work is a modification of the hydroxyapatite column chromatography technique [26]. This technique involves nonspecific interactions between positively-charged calcium ions and negatively-charged phosphate ions on the stationary phase HA resin with negatively-charged carboxyl groups and positively-charged amino groups in the analytes. Multi-modal interaction such as electrostatic adsorption, hydrophobic adsorption, ion exchange or hydrogen bonding may occur between the analytes and HA [36,37]. In addition, a single analyte was added at one time in the present work to compare the interaction equilibrium with other analytes, instead of using the technique for purification purposes. The double peaks shown in the 10-MDP elution profile provides an illustration on how impurities in the commercial 10-MDP (<10% [22]); may be identified. The work presented here suggests that the low molecular weight impurity component of the commercial 10-MDP may be removed by hydroxyapatite column chromatography to produce 10-MDP with a higher degree of purity for fabricating better quality self-etch adhesives. Research in this area is in order.

The performance of column chromatography may be influenced by salts and solvents in the mobile phase. Generally, salts will suppress the electrostatic interactions but enhance hydrophobic interactions. Conversely, organic solvents will suppress hydrophobic interactions but enhance electrostatic interactions [38,39]. Analytes that are retained solely by adsorption are eluted by a suitable organic solvent, while those retained by an ion-exchange mechanism are best desorbed using an acidic or basic eluent that converts the analyte ions back to their molecular form [40]. As reflected by the chromatography results (Fig. 2), when salt buffer was used as the mobile phase, the elution profile of MDA was symmetrical and MDA was 100% recovered. Conversely, the elution profile of 10-MDP (second peak) was asymmetrical and only 36.5% of the 10-MDP eluded from the column. When ethanol was used as the mobile phase, limited 10-MDP (18.9%) or its analog, MDA (33.5%) were recovered. These elution profiles provide hints with respect to the very complicated, mobile-phase dependent interactions between the tested phosphoric acid ester monomers and the stationary phase (i.e. mineralized dentin).

The chromatography results are not in contradiction with the chemoanalytic results. The FTIR, ^{31}P MAS-NMR and XPS specimens were prepared with 15% solution of the phosphoric acid ester monomers, which are much more concentrated than the tracers employed in the chromatography part of the experiments. After reaction, the HA specimens were further washed with ethanol, which may not be able to desorb all the reaction products or unreacted resin monomers. Emergence of new FTIR absorbance peaks at 958 cm^{-1} for the 10-MDP-treated HA spectrum (Fig. 3a), and 982 cm^{-1} on the MDA-treated HA spectrum (Fig. 3b) probably represent $\nu_{3/1}(PO_4)$ P—O stretch of the newly-formed phosphate salts, although definitive assignments of these new peaks were difficult. The weak peak at ~730 cm^{-1} on the 10-MDP-treated HA spectrum (Fig. 3a) may be assigned to P—O—P linear bond formation (confirmed by unpublished NMR examination data).

The FTIR results were also validated by the XPS results (Table 1). The Ca/P ratio was lower for 10-MDP-treated HA compared with MDA-treated HA because of the increase in P percentage caused by monomer adsorption. The C/Ca and O/Ca ratios increased for 10-MDP-treated HA compared to untreated HA because of the adsorption of 10-MDP on HA. High resolution C 1s scans of HA treated with 10-MDP for 30 s or 30 min show that in the absence of a displacement agent that displaces the adsorbed 10-MDP, the phosphoric acid ester monomer remained strongly attached to the HA surface. Although there was initial adsorption of MDA to HA, this interaction is unstable because of the disappearance of the —COO peak characteristic of MDA after 30 min of treatment. Based on the ^{31}P MAS NMR results, disappearance of the ester peak on prolonged interaction of MDA with HA may be caused by MDA desorption during formation of the $CaHPO_4{\cdot}2H_2O$ salt.

The second hypothesis that "there is no difference in the capability of both phosphoric acid ester monomer to produce nanolayering on the dentin surface" has to be rejected. As reflected by the contact angle result and pH measurement, the analog molecule MDA is more hydrophilic and more soluble in water than 10-MDP, and the former is more acidic when solvated in the ethanol-water mixture. The structure of the spacer group may account for the absence of nanolayering in MDA primer-treated dentin. The poly-(propylene glycol) spacer group in MDA is less hydrophobic than the methylene spacer in 10-MDP. Thus, the amphiphilic property of the MDA is not as evident as the 10-MDP monomer. The properties of the resin monomers were reflected in the TEM images resin-dentin interfaces; similar hybrid layer thickness (about 0.5–1.0 μm) was observed. Nanolayering was identified in the gray layer formed above the hybrid layer created by 10-MDP priming. The gray layer was believed to be 10-MDP-calcium salt deposition [19]; this layer was absent in the resin-dentin interface created by MDA. The TEM findings were further supported by the thin-film XRD results. The 10-MDP primed dentin specimens exhibited characteristic peaks of 10-MDP-calcium salt while the MDA primed dentin surface did not exhibit such peaks.

The third hypothesis that "nanolayering of phosphoric acid ester monomer-calcium salts is unstable after water aging and does not contribute to the resin-dentin bond durability" cannot be rejected. Although nanolayering features were ubiquitously identified in the 10-MDP primer-treated dentin interface after one year of water-aging, its bond strength decreased significantly after water aging. There was no significant difference in tensile bond strength values between 10-MDP primed dentin and MDA-primed dentin, both at 24 h and after one year of water-aging. Failure modes of both monomer-bonded samples were predominantly mixed failure. Because the nanolayering structures were protected by a comparatively hydrophobic resin coating (DE Bonding Resin), its resistance to dissolution after water aging is easy to comprehend. Nevertheless, the contribution of nanolayering to resin-dentin bond stability is not as obvious as what was previously proposed [17]. Nanolayering is sparsely identified in resin-dentin interfaces produced by commercial 10-MDP-containing adhesives (e.g. Clearfil SE Bond 2, Kuraray Medical Inc., Tokyo, Japan) [19]. However, the durability of these adhesives had been shown to be excellent, which serves as indirect evidence of limited contribution of nanolayering to bond durability. Aged Clearfil SE Bond 2 specimens showed negligible bond strength drop under the same experimental conditions after one year of water aging (unpublished data). A possible explanation for the decline in bond strength associated with primers containing only 10-MDP may lie in the weak connection between the 10-MDP-Ca salt deposits and the dentin surface. Conceptually, one may consider 10-MDP-Ca salt deposits as a specific type of organic-inorganic hybrid fillers produced *in-situ* during dentin bonding. In resin composites, silica and glass fillers are silanized with methacryloxy silanes to enable them to bond to the methacrylate resin matrix. In the case of 10-MDP-Ca salts, the inward facing of the methacrylate groups of two 10-

MDP molecules may drastically reduce the number of freely available methacryloxy functionalities for coupling to the resin matrix.

Hydroxyapatite is the major mineral phase of dentin. The apatite surface is covered with a highly-ordered bound water layer [41]. This surface water layer provides an efficient proton pool for various adsorbed ions and terminal chemical groups derived from the crystalline phase, such as P—OH (protonated or unprotonated) and Ca—OH groups [42–44]. When mineralized dentin is treated with an acidic primer, apatite dissolution occurs. Although the step-by-step reaction mechanism remains unclear, 8 models have been proposed to explain the processes involved. Dissolution kinetics may be influenced by concentration of acid, ionic strength, solution undersaturation, pH, temperature or crystal dimensions [45]. Generally, the reaction occurs on a diffusion basis: diffusion of chemical reagents (hydronium ions and anions of acid A^{n-}) from bulk solution to the solid/liquid interface, and diffusion of reaction product (Ca^{2+}, $PO4^{3-}$ and OH^{-}) back into the bulk solution [46]. Interaction between calcium cations and adsorbed anions of acid probably happens on the apatite surface as an intermediate stage of the reaction, which results in breaking of surface ≡O—Ca bonds and detachment of calcium-anion salt followed by their diffusion away from mineral surface [46]. In the present situation, adsorption of phosphate anions on HA may involve an ion exchange process (with Ca^{2+}) or hydrogen bonding (with P—OH group), and possibly covalent pyrophosphate formation [47,48].

Based on the adsorption behavior of some carboxylic acids (e.g. oxalic acid) on the apatite surface, the adhesion-decalcification concept (AD concept) was developed and expanded to the interpretation of the effects of other phosphate ester functional monomers on HA [4,5]. The AD concept emphasizes the importance of ionic bond formation between the acid anion and lattice Ca^{2+} ions on the apatite surface [4,49]. As shown by the ability of adsorbed 10-MDP to be slowly eluted from mineralized dentin in the chromatography experiment, the extent and stability of this ion-exchange adsorption require further investigations before the AD concept of chemical bonding may be justified as a mechanism for achieving long-term stable adhesion to dentin. As a matter of fact, oxalic acid can etch the dentin surface and reacts with calcium ions in the smear layer to produce an insoluble calcium oxalate salt on the dentin surface, which replaces the original smear layer with an artificial smear layer [50,51]. This may also be true for 10-MDP-Ca salt because the nanolayering structures were mostly identified above the hybrid layer and form a more or less distinctive gray salt layer in the TEM images.

In acidic solutions, oxalate or phosphate anion would probably react with the released Ca^{2+} ions rather than adsorbing onto the apatite surface, because of non-equivalent adsorption of H^{+} and anion caused by differences in size and mobility [52]. Salt deposition after acid-etching reaction is dependent upon the pH change of the aqueous environment and the solubility product constant (k_{sp}) of the formed salt species. Loose deposition does not necessarily imply the existence of chemical affinity on a hard tissue surface. Although several kinds of calcium salts have been proposed after 10-MDP reacted with dentin or enamel powder, the stability and solubility of these calcium salts have yet to be identified. Because of these issues, the contribution of phosphoric acid ester monomer-calcium salt deposition in the hybrid layer on the durability of resin-dentin bonds remains controversial.

Although the contribution of chemical bonding to the overall bonding durability requires further investigation, recent findings indicate that 10-MDP has relatively stable interaction with collagen [53]. In specific experimental setups, immobilized 10-MDP was found to induce limited extrafibrillar and intrafibrillar mineralization of collagen fibrils [54]. These findings shed light on the potential role of 10-MDP-calcium salt formation on remineralization of poorly-infiltrated collagen scaffold in the hybrid layer and merit more in-depth investigations.

5. Conclusion

Within the limits of the present study, it may be concluded that the claim that nanolayering of 10-MDP-Ca salts is responsible for the durability of resin-dentin bonds created by self-etching 10-MDP-containing dentin adhesives cannot be justified. The 10-MDP-Ca salts may be viewed upon as a highly unique type of organic-inorganic hybrid fillers created *in-situ* during the application of 10-MDP to dentin, in the absence of other resinous components that interfere with the phenomenological expression of nanolayering. Complete elution of the phosphoric acid ester monomer from mineralized dentin powder in the column chromatography experiments using ethanol-water mobile phase to simulate the solvent mixture employed in most 10-MDP-containing dentin adhesives further challenges the previously proposed adhesion-decalcification concept that utilizes chemical bonding of phosphoric acid ester monomers to apatite as a bonding mechanism in 10-MDP containing dentin adhesives.

Acknowledgments

This work was supported by grant 2015AA020942 from National High Technology Research and Development Program of China, grant 81400555 from National Nature Science Foundation, grant Z14110000514016 from Beijing Municipal Science & Technology Commission Project, and program IRT13051 from Changjiang Scholars and Innovative Research Team in University. All authors declared no conflict of interest associated with this work.

References

[1] D.H. Pashley, F.R. Tay, L. Breschi, L. Tjäderhane, R.M. Carvalho, M. Carrilho, A. Tezvergil-Mutluay, State of the art etch-and-rinse adhesives, Dent. Mater. 27 (2011) 1–16.
[2] B. Van Meerbeek, K. Yoshihara, Y. Yoshida, A. Mine, J. De Munck, K.L. Van Landuyt, State of the art of self-etch adhesives, Dent. Mater. 27 (2011) 17–28.
[3] R.M. Carvalho, A.P. Manso, S. Geraldeli, F.R. Tay, D.H. Pashley, Durability of bonds and clinical success of adhesive restorations, Dent. Mater. 28 (2012) 72–86.
[4] Y. Yoshida, B. Van Meerbeek, Y. Nakayama, M. Yoshioka, J. Snauwaert, Y. Abe, P. Lambrechts, G. Vanherle, M. Okazaki, Adhesion to and decalcification of hydroxyapatite by carboxylic acids, J. Dent. Res. 80 (2001) 1565–1569.
[5] Y. Yoshida, K. Nagakane, R. Fukuda, Y. Nakayama, M. Okazaki, H. Shintani, S. Inoue, Y. Tagawa, K. Suzuki, J. De Munck, B. Van Meerbeek, Comparative study on adhesive performance of functional monomers, J. Dent. Res. 83 (2004) 454–458.
[6] D. Fukegawa, S. Hayakawa, Y. Yoshida, K. Suzuki, A. Osaka, B. Van Meerbeek, Chemical interaction of phosphoric acid ester with hydroxyapatite, J. Dent. Res. 85 (2006) 941–944.
[7] Z. Zhang, X. Wang, L. Zhang, B. Liang, T. Tang, B. Fu, M. Hannig, The contribution of chemical bonding to the short- and long-term enamel bond strengths, Dent. Mater. 29 (2013) e103–e112.
[8] V.P. Feitosa, S. Sauro, F.A. Ogliari, A.O. Ogliari, K. Yoshihara, C.H. Zanchi, L. Correr-Sobrinho, M.A. Sinhoreti, A.B. Correr, T.F. Watson, B. Van Meerbeek, Impact of hydrophilicity and length of spacer chains on the bonding of functional monomers, Dent. Mater. 30 (2014) e317–e323.
[9] K. Yoshihara, Y. Yoshida, S. Hayakawa, N. Nagaoka, Y. Torii, A. Osaka, K. Suzuki, S. Minagi, B. Van Meerbeek, K.L. Van Landuyt, Self-etch monomer-calcium salt deposition on dentin, J. Dent. Res. 90 (2011) 602–606.
[10] V.P. Feitosa, F.A. Ogliari, B. Van Meerbeek, T.F. Watson, K. Yoshihara, A.O. Ogliari, M.A. Sinhoreti, A.B. Correr, G. Cama, S. Sauro, Can the hydrophilicity of functional monomers affect chemical interaction, J. Dent. Res. 93 (2014) 201–206.
[11] M. Sarr, A.W. Kane, J. Vreven, A. Mine, K.L. Van Landuyt, M. Peumans, P. Lambrechts, B. Van Meerbeek, J. De Munck, Microtensile bond strength and interfacial characterization of 11 contemporary adhesives bonded to bur-cut dentin, Oper. Dent. 35 (2010) 94–104.
[12] M. Peumans, J. De Munck, K.L. Van Landuyt, B. Van Meerbeek, Thirteen-year randomized controlled clinical trial of a two-step self-etch adhesive in non-carious cervical lesions, Dent. Mater. 31 (2015) 308–314.

[13] S. Inoue, K. Koshiro, Y. Yoshida, J. De Munck, K. Nagakane, K. Suzuki, H. Sano, B. Van Meerbeek, Hydrolytic stability of self-etch adhesives bonded to dentin, J. Dent. Res. 84 (2005) 1160–1164.
[14] H. Iwai, N. Nishiyama, Effect of calcium salt of functional monomer on bonding performance, J. Dent. Res. 91 (2012) 1043–1048.
[15] H. Takahashi, Effect of calcium salt of 10-methacryloyloxydecyl dihydrogen phosphate produced on the bond durability of one-step self-etch adhesive, Dent. Mater. J. 33 (2014) 394–401.
[16] Y. Yokota, N. Nishiyama, Determination of molecular species of calcium salts of MDP produced through decalcification of enamel and dentin by MDP-based one-step adhesive, Dent. Mater. J. 34 (2015) 270–279.
[17] K. Yoshihara, Y. Yoshida, N. Nagaoka, D. Fukegawa, S. Hayakawa, A. Mine, M. Nakamura, S. Minagi, A. Osaka, K. Suzuki, B. Van Meerbeek, Nano-controlled molecular interaction at adhesive interfaces for hard tissue reconstruction, Acta Biomater. 6 (2010) 3573–3582.
[18] Y. Yoshida, K. Yoshihara, N. Nagaoka, S. Hayakawa, Y. Torii, T. Ogawa, A. Osaka, B. Van Meerbeek, Self-assembled nano-layering at the adhesive interface, J. Dent. Res. 91 (2012) 376–381.
[19] F. Tian, L. Zhou, Z. Zhang, L. Niu, L. Zhang, C. Chen, J. Zhou, H. Yang, X. Wang, B. Fu, C. Huang, D.H. Pashley, F.R. Tay, Paucity of nanolayering in resin-rentin interfaces of MDP-based adhesives, J. Dent. Res. 95 (2016) (2015) 380–387.
[20] K. Yoshihara, Y. Yoshida, S. Hayakawa, N. Nagaoka, M. Irie, T. Ogawa, K.L. Van Landuyt, A. Osaka, K. Suzuki, Nanolayering of phosphoric acid ester monomer on enamel and dentin, Acta Biomater. 7 (2011) 3187–3195.
[21] Y. Yoshida, K. Yoshihara, S. Hayakawa, N. Nagaoka, T. Okihara, T. Matsumoto, S. Minagi, A. Osaka, K.L. Van Landuyt, B. Van Meerbeek, HEMA inhibits interfacial nano-layering of the functional monomer MDP, J. Dent. Res. 91 (2012) 1060–1065.
[22] K. Yoshihara, N. Nagaoka, T. Okihara, M. Kuroboshi, S. Hayakawa, Y. Maruo, G. Nishigawa, J. De Munck, Y. Yoshida, B. Van Meerbeek, Functional monomer impurity affects adhesive performance, Dent. Mater. 31 (2015) 1493–1501.
[23] K. Yoshihara, Y. Yoshida, N. Nagaoka, S. Hayakawa, T. Okihara, J. De Munck, Y. Maruo, G. Nishigawa, S. Minagi, A. Osaka, B. Van Meerbeek, Adhesive interfacial interaction affected by different carbon-chain monomers, Dent. Mater. 29 (2013) 888–897.
[24] K. Yoshihara, Y. Yoshida, S. Hayakawa, N. Nagaoka, S. Kamenoue, T. Okihara, T. Ogawa, M. Nakamura, A. Osaka, B. Van Meerbeek, Novel fluoro-carbon functional monomer for dental bonding, J. Dent. Res. 93 (2014) 189–194.
[25] N. Moszner, U. Salz, J. Zimmermann, Chemical aspects of self-etching enamel-dentin adhesives: a systematic review, Dent. Mater. 21 (2005) 895–910.
[26] S. Hjerten, O. Levin, A. Tiselius, Protein chromatography on calcium phosphate columns, Acta Biochem. Biophys. 65 (1956) 132–155.
[27] M. Takahashi, M. Nakajima, J. Tagami, D.L. Scheffel, R.M. Carvalho, A. Mazzoni, M. Cadenaro, A. Tezvergil-Mutluay, L. Breschi, L. Tjäderhane, S.S. Jang, F.R. Tay, K.A. Agee, D.H. Pashley, The importance of size-exclusion characteristics of type I collagen in bonding to dentin matrices, Acta Biomater. 9 (2013) 9522–9528.
[28] A.D. Loguercio, L.P. Barroso, R. Grande, A. Reis, Comparison of intra and intertooth resin-dentin bond strength variability, J. Adhes. Dent. 7 (2005) 151–158.
[29] N. Charadram, C. Austin, P. Trimby, M. Simonian, M.V. Swain, N. Hunter, Structural analysis of reactionary dentin formed in response to polymicrobial invasion, J. Struct. Biol. 181 (2013) 207–222.
[30] Z.R. Hinedi, S. Goldberg, A.C. Chang, J.P. Yesinowski, A ^{31}P and ^{1}H MAS NMR study of phosphate sorption on calcium carbonate, J. Colloid Interface Sci. 152 (1992) 141–160.
[31] Z.Q. He, W. Honeycutt, B.S. Xing, R.W. McDowel, P.J. Pellechia, T.Q. Zhang, Solid-state Fourier transform infrared and ^{31}P nuclear magnetic resonance spectral features of phosphate compounds, Soil Sci. 172 (2007) 501–515.
[32] Y. Yoshida, B. Van Meerbeek, Y. Nakayama, J. Snauwaert, L. Hellemans, P. Lambrechts, G. Vanherle, K. Wakasa, Evidence of chemical bonding at biomaterial-hard tissue interfaces, J. Dent. Res. 79 (2000) 709–714.
[33] H.B. Lu, C.T. Campbell, D.J. Graham, B.D. Ratner, Surface characterization of hydroxyapatite and related calcium phosphates by XPS and TOF-SIMS, Anal. Chem. 72 (2000) 2886–2894.
[34] G.N. Raikar, J.L. Ong, L.C. Lucas, Hydroxyapatite characterized by XPS, Surf. Sci. Spectra 4 (1996) 9–13.
[35] A. Frassetto, L. Breschi, G. Turco, G. Marchesi, R. Di Lenarda, F.R. Tay, D.H. Pashley, M. Cadenaro, Mechanisms of degradation of the hybrid layer in adhesive dentistry and therapeutic agents to improve bond durability – a literature review, Dent. Mater. 32 (2015) e41–e53.
[36] E. Schröder, T. Jönsson, L. Poole, Hydroxyapatite chromatography: altering the phosphate-dependent elution profile of protein as a function of pH, Anal. Biochem. 313 (2003) 176–178.
[37] L.J. Cummings, M.A. Snyder, K. Brisack, Protein chromatography on hydroxyapatite columns, Methods Enzymol. 463 (2009) 387–404.
[38] B.K. Glód, Ion exclusion chromatography: parameters influencing retention, Neurochem. Res. 22 (1997) 1237–1248.
[39] T. Arakawa, Y. Kita, D. Ejima, P. Gagnon, Solvent modulation of column chromatography, Protein Pept. Lett. 15 (2008) 544–555.
[40] J.S. Frit, M. Macka, Solid-phase trapping of solutes for further chromatographic or electrophoretic analysis, J. Chromatogr. A 902 (2000) 137–166.
[41] W. Zhao, Z. Xu, Y. Yang, N. Sahai, Surface energetics of the hydroxyapatite nanocrystal-water interface: a molecular dynamics study, Langmuir 30 (2014) 13283–13292.
[42] S. Cazalbou, C. Combes, D. Eicherta, C. Reya, Adaptive physico-chemistry of bio-related calcium phosphates, J. Mater. Chem. 14 (2004) 2148–2153.
[43] M. Jarlbring, D.E. Sandström, O.N. Antzutkin, W. Forsling, Characterization of active phosphorus surface sites at synthetic carbonate-free fluorapatite using single-pulse ^{1}H, ^{31}P, and ^{31}P CP MAS NMR, Langmuir 22 (2006) 4787–4792.
[44] J. Kolmas, A. Slósarczyk, A. Wojtowicz, W. Kolodziejski, Estimation of the specific surface area of apatites in human mineralized tissues using ^{31}P MAS NMR, Solid State Nucl. Magn. Reson. 32 (2007) 53–58.
[45] S.V. Dorozhkin, Dissolution mechanism of calcium apatites in acids: a review of literature, World J. Methodol. 2 (2012) 1–17.
[46] S.V. Dorozhkin, Surface reactions of apatite dissolution, J. Colloid Interface Sci. 191 (1997) 489–497.
[47] D.N. Misra, Adsorption from solutions on synthetic hydroxyapatite: nonaqueous vs. aqueous solvents, J. Biomed. Mater. Res. 48 (1999) 848–855.
[48] C.D. Susan, Y.F. Alexander, Covalent surface modification of calcium hydroxyapatite ysing n-alkyl- and n-fluoroalkylphosphonic acids, Langmuir 19 (2003) 7904–7910.
[49] M. Yoshioka, Y. Yoshida, S. Inoue, P. Lambrechts, G. Vanherle, Y. Nomura, M. Okazaki, H. Shintani, B. Van Meerbeek, Adhesion/decalcification mechanisms of acid interactions with human hard tissues, J. Biomed. Mater. Res. 59 (2002) 56–62.
[50] D.H. Pashley, S.E. Galloway, The effects of oxalate treatment on the smear layer of ground surfaces of human dentine, Arch. Oral Biol. 30 (1985) 731–737.
[51] C.K. Yiu, N.M. King, B.I. Suh, L.J. Sharp, R.M. Carvalho, D.H. Pashley, F.R. Tay, Incompatibility of oxalate desensitizers with acidic, fluoride-containing total-etch adhesives, J. Dent. Res. 84 (2005) 730–735.
[52] A.E. Nielsen, Transport control in crystal growth from solution, Croat. Chem. Acta 53 (1980) 255–279.
[53] N. Hiraishi, N. Tochio, T. Kigawa, M. Otsuki, J. Tagami, Monomer-collagen interactions studied by saturation transfer difference NMR, J. Dent. Res. 92 (2013) 284–288.
[54] H. Nurrohman, S. Nakashima, T. Takagaki, A. Sadr, T. Nikaido, Y. Asakawa, M. Uo, S.J. Marshall, J. Tagami, Immobilization of phosphate monomers on collagen induces biomimetic mineralization, Biomed. Mater. Eng. 25 (2015) 89–99.